Disordered Bose-Einstein Condensates in Quasi-One-Dimensional Magnetic Microtraps

Daw-Wei Wang, Mikhail D. Lukin, and Eugene Demler
Physics Department, Harvard University, Cambridge, Massachusetts 02138, USA
(Received 16 July 2003; published 18 February 2004)

We analyze the effects of a random magnetic potential in a microfabricated waveguide for ultracold atoms. We find that the shape and position fluctuations of a current carrying wire induce a strong Gaussian correlated random potential with a length scale set by the atom-wire separation. The theory is used to explain quantitatively the observed fragmentation of the Bose-Einstein condensates in atomic waveguides. Furthermore, we show that nonlinear dynamics can be used to provide important insights into the nature of the strongly fragmented condensates. We argue that a quantum phase transition from the superfluid to the insulating Bose glass phase may be reached and detected under the realistic experimental conditions.

DOI: 10.1103/PhysRevLett.92.076802 PACS numbers: 73.21.Hb, 03.75.Lm, 05.30.Jp

Several groups have recently reported realizations of quasi-one-dimensional (Q1D) Bose-Einstein condensates (BEC) in the magnetic waveguides for atoms created by the microfabricated wires (magnetic traps on microchips) [1–4]. A surprising feature is the presence of fragmentation: a random modulation of the atomic density in the axial direction [2–4]. For smaller atom-wire separation the fragmentation is enhanced and its characteristic length scale decreases. Determination of the origin and the properties of the observed density modulation is essential for understanding atomic condensates on microchips and for developing atom-optical microfabricated devices. Several observations suggest that the wire shape and position fluctuations are the primary origin of the fragmentation [2–4]; however, a detailed theoretical understanding of these phenomena is still lacking [5].

In this Letter, we use a first-principles microscopic calculation to demonstrate that a small meandering of the wire leads to a strong random potential in a magnetic microtrap [6]. We show that, even when the wire fluctuations have no intrinsic length scale, the disorder magnetic potential in the waveguide is a Gaussian correlated random potential with a correlation function that is strongly peaked at a finite wave vector and vanishes for small and large wave vectors. The characteristic length scale is set by the atom-wire distance d. This theoretical model is used to quantitatively explain the experimental results. We then study the properties of the Q1D atomic BEC in the regime of strong fragmentation. Some of the most striking manifestations of this strong disorder limit appear in the nonlinear dynamics of the fragmented condensate, including a chaos and a self-trapping of the excitations. We argue that the quantum phase transition between the superfluid (SF) and the insulating Bose glass (BG) phases can be achieved and detected under realistic experimental conditions.

Neutral atoms with a magnetic dipole moment $\boldsymbol{\mu}_a$ antialigned with respect to the magnetic field $\mathbf{B}$ experience a potential $U(\mathbf{r}) = \mu_a|\mathbf{B}(\mathbf{r})|$, so they can be confined near a field minimum [1]. A typical microtrap setup is shown in Fig. 1. The waveguide is located at a distance $d = 2I_0/cB_\perp$ from the wire center, where the azimuthal magnetic field created by the wire cancels out the transverse bias field $B_\perp$. The longitudinal confinement can be provided by the additional magnetic field gradients applied parallel to the wire.

We now discuss a random magnetic potential along the center of the waveguide caused by the shape and position fluctuations of the current carrying wire. Let $f_{L/R}(z)$ be the deviations of the wire's left/right boundaries from their ideal positions at $y = \mp W_0/2$. Changes in the wire height provide a much smaller contribution to the fluctuating magnetic field, so we neglect them throughout this Letter. In a steady state the deviation of the current density $\delta\mathbf{J}(y, z)$ from its average value J_0 satisfies the charge conservation condition $\partial\delta J_y/\partial y + \partial\delta J_z/\partial z = 0$. If we simultaneously assume a constant conductivity throughout the wire, the current is also vorticity

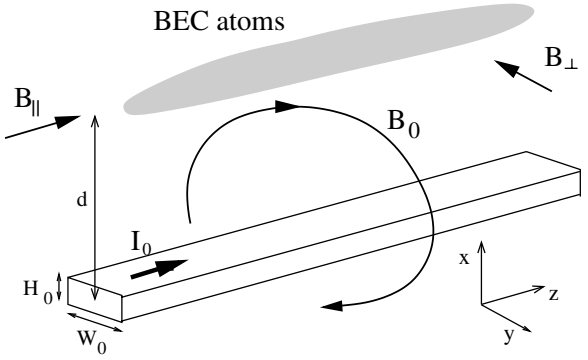

FIG. 1. Typical setup of a magnetic microtrap: A current I_0 flowing in a microfabricated copper conductor and a perpendicular bias field $B_\perp$ form a magnetic waveguide for atoms. An offset field $B_\parallel$ applied parallel to the wire reduces loss processes near the magnetic field minimum.

 0031-9007/04/92(7)/076802(4)$22.50

free, $\partial\delta J_z/\partial y - \partial\delta J_y/\partial z = 0$. Boundary conditions for $\delta\mathbf{J}(y, z)$ follow from the requirement that no current flows out of the wire. Assuming small fluctuations of the wire ($|f_{L/R}(z)| \ll W_0$ and $|\partial f_{L/R}/\partial z| \ll 1$), we have $\delta J_y(\mp W_0/2, z)/J_0 = \partial f_{L/R}(z)/\partial z$. It is convenient to introduce an auxiliary scalar potential $G_J(y, z)$, such that $\delta J_y = J_0 \partial G_J/\partial z$ and $\delta J_z = -J_0 \partial G_J/\partial y$. The function $G_J(y, z)$ satisfies the Laplace equation in the interior of the wire and has Dirichlet boundary conditions at $y = \mp W_0/2$. Using separation of variables, we find

$$G_J(y, z) = \frac{2}{\pi}\int \frac{e^{ikz}dk}{\sinh(kW_0)} \times [\cosh(ky)\sinh(kW_0/2)f_k^+ + \sinh(ky)\cosh(kW_0/2)f_k^-], \quad (1)$$

where $f_k^{\pm} \equiv \frac{1}{2}\int_{-\infty}^{\infty} dz e^{ikz}(f_R(z) \pm f_L(z))$ are the Fourier components of the wire position and width fluctuations. The fluctuating part of the magnetic field can be found from the Biot-Savarat law:

$$\delta\mathbf{B}(\mathbf{r}) = \frac{J_0}{c}\int_{-\infty}^{\infty} dz' \int_{-(H_0/2)}^{H_0/2} dx' \int_{-(W_0/2)}^{W_0/2} dy' G_J(y', z') \times \left\{ -\frac{2(x-x')^2 - (y-y')^2 - (z-z')^2}{[(x-x')^2 + (y-y')^2 + (z-z')^2]^{5/2}}\hat{\mathbf{x}} + \frac{-3(x-x')(y-y')\hat{\mathbf{y}}}{[(x-x')^2 + (y-y')^2 + (z-z')^2]^{5/2}} + \frac{-3(x-x')(z-z')\hat{z}}{[(x-x')^2 + (y-y')^2 + (z-z')^2]^{5/2}} \right\}. \quad (2)$$

To obtain Eq. (2) we performed the integration by parts, which led to a cancellation of the contributions from the $y \in (-\frac{W_0}{2} + f_L(z), -\frac{W_0}{2})$ and $y \in (\frac{W_0}{2}, \frac{W_0}{2} + f_R(z))$ regions. The leading order random potential comes from the z component of the magnetic field, $\delta U(\mathbf{r}) = \pm\mu_a \delta B_z(d, 0, z)$, if the condensate width is much smaller than d (the $\pm$ sign is the orientation of the offset field $B_\parallel$). From Eqs. (1) and (2) one can see that only the wire position fluctuations f^+ contribute to $\delta U(\mathbf{r})$ at this order.

To elucidate the nature of the resulting random potential, we compute the correlation function $\Delta_k = \int dz e^{ik(z-z')}\langle\delta U(z)\delta U(z')\rangle_{\text{dis}}$, where $\langle\cdots\rangle_{\text{dis}}$ is disorder ensemble average. Assuming $H_0 \ll d$ (this condition is typically satisfied in experiments), we obtain

$$\Delta_k = \left(\frac{2I_0\mu_a}{c}\right)^2 \frac{(kd)^4}{d^4} |K_1(kd)D(kW_0, kd)|^2 F_k,$$

where $F_k = \int dz\, e^{-ik(z-z')}\langle f^+(z)f^+(z')\rangle_{\text{dis}}$, and

$$D(x, y) = \frac{2\sinh(x/2)}{x\sinh(x)K_1(y)} \sum_{n=0}^{\infty} \frac{(-1)^n}{n!(2y)^n} K_{n+1}(y) \times [\gamma(2n+1, x/2) - \gamma(2n+1, -x/2)]. \quad (3)$$

$K_n(x)$ is the Bessel function of the second kind, and $\gamma(n, x) \equiv \int_0^x dx' x'^{n-1} e^{-x'}$ is the incomplete Gamma function. The strength of the disorder potential can be defined as $u_s^2 \equiv \langle\delta U(z)\delta U(z)\rangle_{\text{dis}} = \int_{-\infty}^{\infty} \frac{dk}{2\pi}\Delta_k$. For $d \gg W_0$ we obtain

$$u_s \sim \frac{2I_0\mu_a}{cd}\left(\frac{F_0}{d^3}\right)^{1/2}. \quad (4)$$

Fixing current I_0 we find $u_s \sim d^{-5/2}$, which is close to the experimentally observed $u_s \sim d^{-2.2}$ [2]. We can also estimate the magnitude of the random potential: If $\delta f \sim 0.1\ \mu$m is the scale of the wire position fluctuation and $\xi \sim 100\ \mu$m is the appropriate correlation length, then $u_s \sim \mu_a B_\perp(\delta f\, \xi^{1/2}/d^{3/2}) \sim$ kHz for $B_\perp \sim 1$ G and $d \sim 100\ \mu$m. This value is comparable to a typical value of the BEC chemical potential and explains the strong fragmentation effects observed in magnetic microtraps [2–4,6].

In Fig. 2(a) we show Δ_k computed for the white noise fluctuations of the wire center position. It peaks at $k_0 \approx 1.3/d$ and vanishes in the $k = 0$ and $k = \infty$, showing a characteristic length scale d. Long wavelength fluctuations are suppressed because a uniform shift of the random potential does not lead to a parallel (z) component of the magnetic field. In the inset in Fig. 2(a), we demonstrate how the random magnetic potential is modified when the wire fluctuations have an intrinsic length scale $1/k_1$ (see caption). When the wire fluctuations are short ranged ($k_1 d \gg 1$), the potential fluctuations remain peaked close to $k_0 \sim 1.3/d$, and the length scale of the random potential is set by the atom-wire separation. When the wire fluctuations are longer ranged ($k_1 d < 1$), Δ_k is then peaked at $k \sim k_1$, and the random potential tracks the wire fluctuations. A linear relation between the condensate height and the length scale of the fragmentation was observed in Refs. [3,4]. In Fig. 2(b) we show the calculated condensate density profiles for 10^6 sodium atoms in the Thomas-Fermi approximation using the same wire fluctuations taken from the distribution of the inset in Fig. 2(a). The fragmentation appears for $d \leq 100\ \mu$m (cf. Ref. [3]). We note that the profiles obtained by a white noise potential (i.e., $\Delta_k = \text{const}$) do not have a characteristic length scale and are very *different* from the above results and experiments.

We next consider the new phenomena that emerge in the strong fragmentation regime, where the random potential is appreciably larger than the chemical potential of the atoms so that the tunneling rate for the atoms between the neighboring wells is much smaller than the local confinement frequency. The zero temperature condensate wave function then can be approximated by the tight-binding model [7,8]: $\Phi(z) = \sum_j \sqrt{N_j}\,\phi_j(z)\, e^{iS_j}$, where $\phi_j(z)$ is the localized single particle wave function

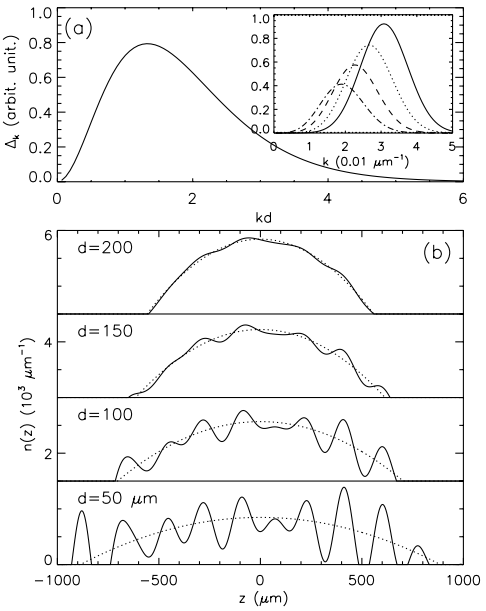

FIG. 2. (a) Correlation function of the random magnetic potential in a microtrap Δ_k, assuming white noise fluctuations of the wire position (i.e., $F_k = \text{const}$). Inset: Δ_k when the wire fluctuations have an intrinsic length scale: $F_k \propto [e^{-(k-k_1)^2\eta_1^2} + e^{-(k+k_1)^2\eta_1^2}]$. We take $2\pi/k_1 = 200$ μm, $\eta_1 = 100$ μm, and $\langle f^+(z)f^+(z)\rangle_{\text{dis}} = (0.1\ \mu\text{m})^2$. Solid to dash-dotted lines correspond to $d = 50$, 100, 150, and 200 μm, respectively. (b) Condensate density profiles with parameters chosen to be close to the values used in the experiments of Ref. [3]. Dotted lines are the results *without* random potential.

(here obtained by solving the on site Gross-Pitaevskii equation), N_j is the number of particles, and S_j is the phase of the minicondensate j. Equations of motion of the minicondensates (i.e., fragments) are given by

$$\dot{S}_j + U_j(N_j - N_j^0) = 0, \tag{5}$$

$$\dot{N}_j + \sum_{\alpha=\pm 1} \tilde{K}_{j,j+\alpha} \sin(S_{j+\alpha} - S_j) = 0, \tag{6}$$

where U_j and N_j^0 are the "charging energy" and the equilibrium number of atoms in the well j; $\tilde{K}_{j,j'} \equiv K_{j,j'}\sqrt{N_j N_{j'}}$ is the "Josephson energy" and $K_{j,j'}$ is a single particle tunneling rate between the wells j and j'. Equation (5) is the Josephson relation between the local chemical potential $\delta\mu_j = U_j(N_j - N_j^0)$ and the phase S_j. Equation (6) describes the charge conservation.

The key properties of such fragmented BEC can be revealed by exciting BEC in the "shaking" experiments. In these experiments one quickly displaces the global confining potential along the waveguide and observes the ensuing motion of the condensate. From the numerical analysis of Eqs. (5) and (6), we identified three types of response of the system to the initial displacement D [see Fig. 3(a)] [9]: (i) For small D only the dipole mode is excited. (ii) As D increases, the dipole mode becomes unstable and many other modes are generated, leading to chaotic behavior. (iii) When D gets even larger, the system is "trapped" in small oscillations around some configuration with strong imbalance of the atom density. The number of atoms in individual wells is not oscillating around the equilibrium values N_j^0, but around some nonuniform density distribution. We call this regime self-trapping of the excitations [10].

The power spectra of the oscillations provide a direct way to identify different types of the dynamical behavior. In regime (i) condensate oscillates at the frequency of the dipole mode and its higher harmonics [see Fig. 3(b)]. In regime (ii) we have a broad distribution of frequencies [see Fig. 3(c)]. In the limit of self-trapping, for every point in the system we have several dominant frequencies and their harmonics [see Fig. 3(d)]. The transition of the system from a dipole mode into a chaotic regime originates from the nonlinearity of Eqs. (5) and (6) and is similar to the modulation instability in optical lattices [8]. For strong disorder the superfluidity are terminated by strong quantum fluctuations and that the system should go into the insulating Bose glass phase (BG) [11]. Therefore, the coherent dipole fluctuations should disappear at the SF/BG transition point, and the self-trapping response should become dominant in the BG phase due to the localized nature of the insulating state. The qualitative phase diagram is shown in Fig. 3(a).

More quantitatively, transition into an insulating state can be estimated by the ratio of the Josephson energy between the neighboring wells to the average charging energy, $Q_j = 8\tilde{K}_{j,j+1}/[(U_j + U_{j+1})/2]$. The SF to the Mott insulator transition in a periodic potential takes

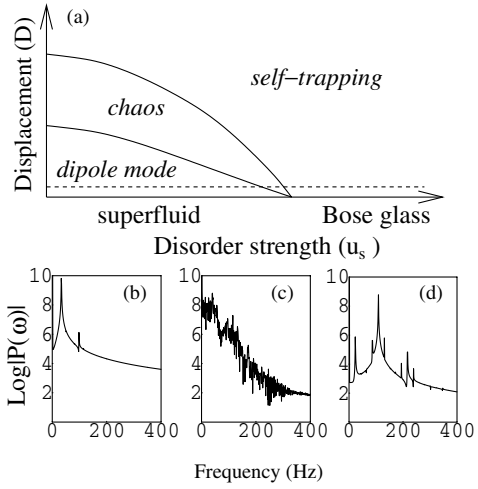

FIG. 3. (a) Schematic dynamical phase diagram of fragmented Q1D BEC in relation to the shaking experiments. The dashed line indicates the minimum displacement to generate an observable density fluctuations (i.e., $\zeta > \zeta_{\text{min}}$). Three types of responses can be identified from the power spectra of the oscillations: (b) dipole mode regime, (c) chaos, and (d) self-trapping. Power spectra are obtained from simulations of a three well system with $\langle N_j\rangle = 10^5$.

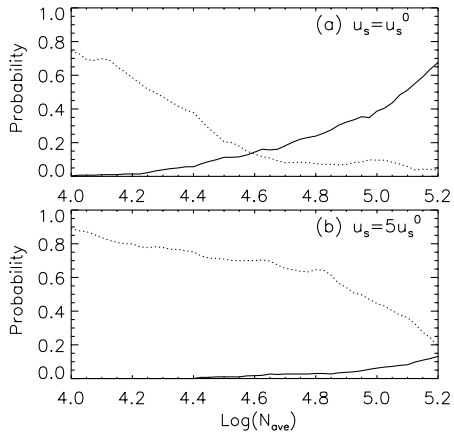

FIG. 4. The dotted line shows the probability $\mathcal{P}(Q<1)$, which is close to zero if the system is in the superfluid regime and is close to one if in the insulating Bose glass phase. The solid line shows the probability that one can observe fluctuations in the number of atoms between the neighboring wells with $\omega_J \geq \omega_{\min}$ and $\zeta \geq \zeta_{\min}$ (see text). When this probability approaches zero, the system will appear self-trapped in the shaking experiments. N_{ave} is the average number of atoms in a single well (minicondensate). Disorder strength for (a) is the same as used in Fig. 2(b) for $d = 100$ μm (denoted to be u_s^0), while it is 5 times stronger in (b).

place when $Q = 1$ in the mean field theory. For a correlated random potential we expect that the SF to the BG phase transition takes place when the probability to have $Q < 1$ in a junction, $\mathcal{P}(Q<1)$, is of the order of 1. In Fig. 4 we show $\mathcal{P}(Q<1)$ as a function of the atom density for two different strengths of the disorder potential (dotted lines). Taking the parameters corresponding to the experiments of Ref. [3] with $d = 100$ μm, we estimate that a system of atoms with $N_{\text{ave}} < 10^4$ per fragment should be in the BG phase.

Naturally, the shaking experiments can be used to identify the SF/BG transition. In practice, a finite lifetime of a condensate limits experimentally measurable Josephson frequencies ω_J to be $\omega_J \geq \omega_{\min}$. Another limiting factor for the experiments comes from the finite density contrast $\zeta = \Delta N/N_0 > \zeta_{\min}$, required for resolving oscillations. The solid curve in Fig. 4 shows the probability of observing a dipole mode or chaotic dynamics for a given disorder strength with the minimum displacement for $\omega_{\min} = 2\pi \times 1$ Hz and $\zeta_{\min} = 0.1$. The observation of the self-trapping transition as a function of the disorder strength at a small D should provide a reasonable estimate of the SF-BG transition point [9], as illustrated by the dashed line in Fig. 3(a). We expect that such dynamical properties and a sharp crossover to the insulating regime are still valid, at least qualitatively, in the temperature regime of current experiments.

In the shaking experiments discussed so far, the random potential was kept fixed and the confining potential was displaced. It would also be interesting to keep the confining potential fixed and oscillate the random potential at some frequency. This would be a direct analog of the Andronikashvilli experiments for superfluid ^{4}He in a disordered medium [12], which provide a direct measure of the superfluid fraction.

In summary, we performed microscopic calculations of a random magnetic potential for the atomic BEC in a microtrap. We showed that a small meandering of the wire is sufficient to explain the experimentally observed fragmentation of the condensates [6]. The response to the trap shaking can be used to study the superfluid properties of the strongly fragmented condensates and to identify the quantum phase transition from superfluid to the insulating Bose glass phase. More generally, our work demonstrates that atoms in the magnetic microtrap are a very promising system for controlled study of one-dimensional disorder problems.

The authors acknowledge useful discussions with E. Altman, E. Heller, D. Nelson, M. Prentiss, and D. E. Pritchard. We especially thank A. E. Leanhardt and S. Kraft for explaining details of the experiments. This work was supported by the NSF (Grants No. DMR-01328074 and No. PHY-0134776), the Sloan and the Packard Foundations, and by Harvard-MIT CUA.

[1] W. Hansel *et al.*, Nature (London) **413**, 498 (2001); J. H. Thywissen *et al.*, Eur. Phys. J. D **7**, 361 (1999); R. Folman *et al.*, Adv. At. Mol. Opt. Phys. **48**, 263 (2002).
[2] S. Kraft *et al.*, J. Phys. B **35**, L469 (2002).
[3] A. E. Leanhardt *et al.*, Phys. Rev. Lett. **89**, 040401 (2002); **90**, 100404 (2003).
[4] J. Fortagh *et al.*, Phys. Rev. A **66**, 041604 (2002).
[5] The thermal fluctuations from the substrate surface are negligible in the present atom-wire distance.
[6] We note that such disorder effects can be neglected in the macroscopic magnetic traps, where the atoms are far away from the wire ($d \sim 1$ cm) and hence the disorder vanishes according to Eq. (4).
[7] M. Kramer *et al.*, Phys. Rev. Lett. **88**, 180404 (2002); F. S. Cataliotti, Science **293**, 843 (2001).
[8] A. Smerzi *et al.*, Phys. Rev. Lett. **89**, 170402 (2002); F. S. Cataliotti *et al.*, cond-mat/0207139.
[9] Note that, in the thermodynamic limit, various regimes may be distinguished only for a bounded disorder, while in a finite system there is no true phase transition—however, one may still observe the sharp crossovers.
[10] Note that the ends of the condensate may be trapped even when the bulk of the system is not.
[11] T. Giamarchi and H. Schulz, Phys. Rev. B **37**, 325 (1988); M. P. A. Fisher *et al.* Phys. Rev. B **40**, 546 (1989).
[12] J. D. Reppy, J. Low Temp. Phys. **87**, 205 (1992); P. A. Crowell *et al.*, Phys. Rev. B **51**, 12 721 (1995).